Nuclear Instruments and Methods in Physics Research B 491 (2021) 52–58

Contents lists available at ScienceDirect

Nuclear Inst. and Methods in Physics Research, B

journal homepage: www.elsevier.com/locate/nimb

Heavy ion radiation and temperature effects on SiC schottky barrier diode

Duowei Wang [a], Rongbin Hu [b], Gang Chen [b], Changqin Tang [c], Yao Ma [a,c], Min Gong [a,c], Qingkui Yu [d], Shuang Cao [d], Yun Li [a,c], Mingmin Huang [a,c], Zhimei Yang [a,c,*]

[a] Key Laboratory for Microelectronics, College of Physics, Sichuan University, Chengdu 610064, China
[b] Science and Technology on Analog Integrated Circuit Laboratory, Chongqing 400060, China
[c] Key Laboratory of Radiation Physics and Technology of Ministry of Education, Sichuan University, Chengdu 610064, China
[d] China Academy of Space Technology, Beijing 100029, China

ARTICLE INFO

Keywords:
SiC schottky barrier diode
Commercial device
Heavy Ions
Irradiation
Temperature dependence

ABSTRACT

The function of a commercial Schottky Barrier Diode (SBD) based on 4H-SiC in an environment of extreme temperature and radiation was assessed. The capacitance-voltage (C-V) and current-voltage (I-V) characteristics of the devices were measured by heavy ions (HIs) irradiation at 3 different fluences and 15 different nodes of temperature. From these measurements, the effective carrier concentration (N_D), reverse current (I_R), series resistance (R_S), ideal factor (n), and Schottky barrier height (SBH) were calculated and analyzed. Obvious increases of N_D and I_R were found and some changes of the electronic characteristics with temperature were enhanced by HIs. After the highest fluence of irradiation, the I_R at low temperature (20 K) was even larger than the I_R at room temperature, which was subjected to lower fluence of irradiation, suggesting risks for aerospace applications. These changes were attributed to defects both at the interface and in the body-substrate induced by irradiation.

1. Introduction

With the development of the aerospace industry, new devices based on semiconductors have been proposed, including many power devices. Considered as a mainstream semiconductor device of the third generation, devices fabricated of silicon carbon (SiC) possess excellent properties, including high thermal conductivity, high breakdown field high saturation velocity of carriers, and much higher band gap than silicon [1–3]. The high band gap limits hole-electron excitement for operation of the devices work in a rich radiation environment such as aerospace, requiring great anti-irradiation property [4]. However, this property has not been verified previously for these devices. Under the Single Event Effect test, SiC-based devices exhibit bad performance by swift heavy ions (SHIs) irradiation damage [5].

When semiconductor devices work in space, the electronic characteristics might change because of the various kinds of particles and the rapidly-changed temperature. There are many reports about irradiation inducing defects in SiC devices, using different radiation sources like electrons [6,7], protons [8], fast neutrons [9], and alpha particles [10–12]. The results revealed variation in the electrical properties of radiated SiC diodes and radiation resistance of these devices that depended on types, energies, flux, fluence, and the absorbed dose of irradiated particles. There are fewer studies of the effects of heavy ions (HIs) irradiation on SiC Schottky Barrier Diodes (SBDs), with most studies examining effects of other sources of radiation or focusing on single event or charge collection effects [13–15]. Singe Event Effects (SEEs) is essential for the function of power devices when they work in radiation environments, but the effects induced by irradiation at the off-state may also affect function of these devices, including changes of the electronic properties. Previous studies relied on Schottky Barriers prepared in the laboratory, which may significantly differ from commercial multi-layer devices. For example, a recent study examined the effects of irradiation by 200 MeV Ag ions on commercial SiC SBD devices. The electronic characteristics were measured at room temperature, and the results indicated the forward current increased with the fluences of irradiation at low bias voltage and significantly decreased at higher bias voltage [16]. The R_S also clearly increased and N_D decreased after irradiation. The changes of electronic characteristics would obviously cause the devices to work in altered states. When such power devices work in aerospace, they would not always be directly exposed to cosmic rays, so the energy of the ions penetrating the devices would be variable. Thus, it is important to examine the changes in function when devices

* Corresponding author at: Key Laboratory for Microelectronics, College of Physics, Sichuan University, Chengdu 610064, China.
E-mail address: yangzhimei@scu.edu.cn (Z. Yang).

https://doi.org/10.1016/j.nimb.2021.01.019
Received 23 September 2020; Received in revised form 20 January 2021; Accepted 31 January 2021
Available online 11 February 2021
0168-583X/© 2021 Elsevier B.V. All rights reserved.

are under irradiation with low energy. In aerospace, the temperature can change rapidly over a large range, and also affect the properties of these devices. Therefore, we have studied commercial SiC SBD devices irradiated with HIs at comparatively low energy and determined the temperature properties after irradiation. The results of this work can guide the application of commercial SiC SBDs applied in an environment that is rich in radiation or experiences extreme temperature changes.

In this study, the effects on commercial 4H-SiC SBDs provided by Cree Inc. were determined. We applied 3 different fluences of 6 MeV Au ions irradiation on these devices and measured the I-V and C-V at 15 different nodes of temperature (20 K-500 K). The relevant parameters were calculated based on the electronic measurements. We found that irradiation by HIs at off-state affected the electronic characteristics of the SBDs when functioning at high temperature. For instance, there was an obvious increase of the forward current at lower forward bias and at reverse bias voltage, suggesting significant risks for application of these devices in a rich-radiation environment. Additionally, a significant decrease of capacitance at reverse bias voltage for temperatures higher than 140 K was observed. At lower temperature, HIs radiation had little effect on reverse capacitance. When power devices work in aerospace, the working temperature range is always very large, and includes high temperature. The results and analysis of the parameters suggest that both body defects and interface defects might be induced by HIs radiation and affect the electronic characteristics.

2. Experiment

In this study, we measured the electronic characteristics before and after 3 fluences of irradiation by HIs irradiation of a commercial 4H-SiC SBD, which is fabricated by Cree Inc. (CSD01060 (600 V, 10 A, active areas estimated to be 0.5 mm^2). To make sure the Au ions penetrate the sensitive layer of the SBDs, the plastic package of the SBDs was removed before HIs application. The SBD with SiC substrate has an Al/W/WTi/Ti metal layer, where the thickness of W/WTi/Ti is 135 nm, 212 nm, and 98 nm, respectively [17]. The irradiation part of the experiment was executed on a 3 MV Tandetron accelerator, characterized as a high-fluence radiation source, at the Institute of Nuclear Science and Engineering at Sichuan University [18]. Irradiation was performed with Au ions of 3 different total fluences: 1E13, 1E14 and 1E15 ions /cm^2, using an influence rate of 5E12 ions/(cm^2 s). Before irradiation, the electronic characteristics were measured using Keysight B2902 for I-V measurement, Agilent B1500A for C-V measurement, and Genius CCS450 for temperature control. I-V and C-V measurements were conducted over a temperature range from 20 K to 500 K, with 15 selected temperature nodes. After irradiation, the same measurements were performed. Analysis showed negligible differences before and after the lowest irradiation, and we discussed the changes in the electronic characteristics of the irradiated devices. Simulations were performed using Stopping and Range of Ions in Matter (SRIM), and the electron energy loss and nuclear energy loss were determined as 12.44 and 6.995 MeV/(mg*cm^2), respectively. The ion projection range was 0.92 μm in SiC material. The plot of electron and nuclear energy loss versus depth of SiC is shown in Fig. 1. (a), and vacancy concentration is shown in Fig. 1 (b). In the plot, it is clearly to find that the electron energy loss is monotone decrease with depth, while the nuclear energy loss increase first and reach the peak at 0.75 μm. Both type of energy loss are end at the position about 1.1 μm. Also, the vacancy concentration appears same regularity with nuclear energy loss. The order of magnitudes of the concentration is about 10^8. Monte Carlo simulation software GEANT4 was also used to simulate the HIs radiation on this structure. We found that the incidence range of Au ions at 6 MeV is about 2074 nm, which means it is hard to pass through the Al layer with thickness about 4 μm.

3. Results and discussion

3.1. Equations to extract parameters

Eq. (1) can be used to calculate N_D and SBH from C-V results [19]. Where C represents capacitance, A represents the junction area, q represents charge of an electron, ε_s represents the dielectric constant, k_0 represents the Boltzmann constant, and V represents the bias voltage.

$$\frac{1}{C^2} = \frac{2}{qA^2 N_D \varepsilon_S}(SBH/q - V - (E_C - E_F)/q - \frac{k_0 T}{q}) \quad (1)$$

Eqs. (2) and (3) can be used to calculate the ideal factor (n_r), which considers series resistance, $SBH_{I\text{-}V}$, and series resistance (R_S) [20]. Where A* represents the Richardson constant, k_0 the Boltzmann constant. These two equations can be used to calculate the n_r and $SBH_{I\text{-}V}$ from the I-V test results.

$$\frac{dV}{dlnI} = R_S I + n_r \frac{k_0 T}{q} \quad (2)$$

$$H = V - n\frac{k_0 T}{q} ln\left(\frac{I}{A^* T^2}\right) = R_S I + n^* SBH \quad (3)$$

3.2. Results of electronic characteristics at room temperature

I-V and C-V measurements were performed at room temperature. Based on the results, the parameters of SBH, N_D and R_S were extracted. Fig. 2a) shows the 1/C^2-V results under 3 fluences, and the fit result of the lowest fluence is shown in Fig. 2 (b). Similarly, Fig. 2. (c) shows the semi-log I-V results and the Fig. 2(d) shows the I-V results in reverse. According to Eq. (1), N_D and $SBH_{C\text{-}V}$ were calculated via 1/C^2-V plots.

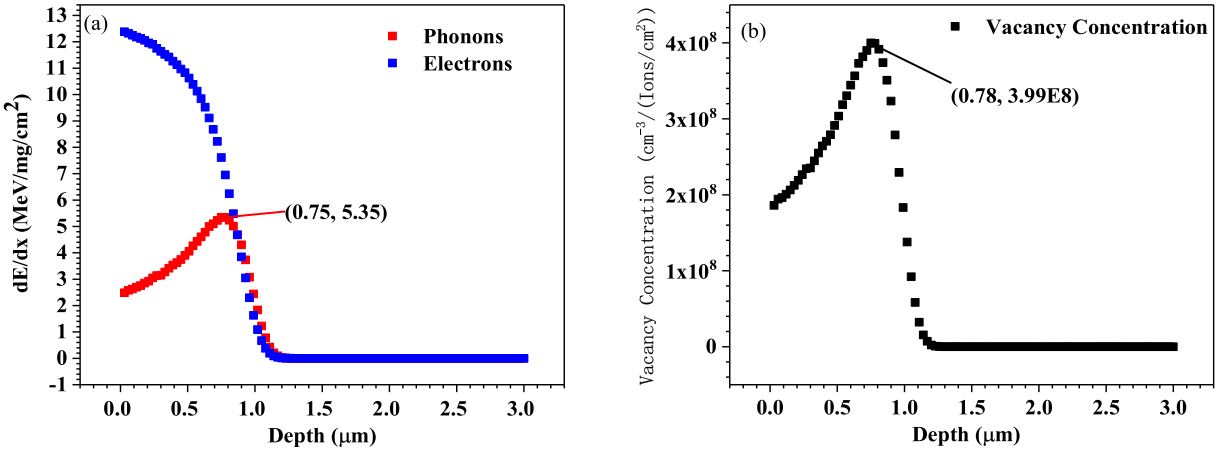

Fig. 1. (a) the electron and nuclear energy loss versus depth. (b) the vacancy concentration versus depth.

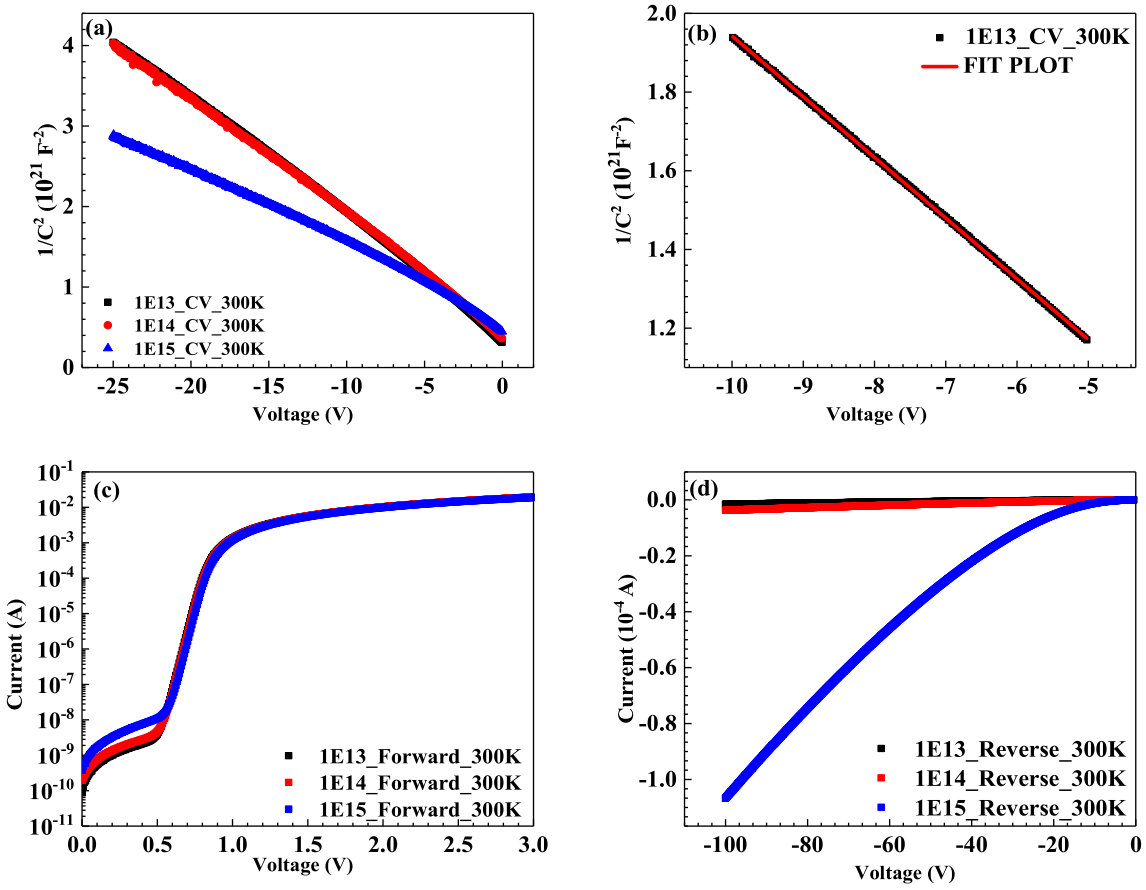

Fig. 2. (a) $1/C^2$-V results (b) $1/C^2$-V fit result after radiation of 1E13 cm-2. (c) ln(I)-V results and (d) reverse I-V results.

The ideal factor was calculated from ln (I)-V fit directly (n) and from Eq. (2) (n_r). Assuming the Richardson constant is 146 A / ($cm^2 \cdot K^2$), Eq. (3) was used to calculate the $SBH_{I\text{-}V}$. The results are shown in Table 1. The fit plot of I-V result at the lowest fluence is shown in Fig. 3.

It is obvious to see that with increasing radiation fluence, some defects were formed to induce the synchronous increase of N_D and SBH, which is the main reason to cause the changes of the I-V and the C-V characteristics. At 300 K, irradiation did not have much of influence on the forward current at higher voltage, but caused increasing current with fluences at lower voltage range.

Radiation might induce defects and interface states in SiC SBD devices, causing SBH extracted from $1/C^2$-V to increase and slight changes in H-I. The N_D and the R_S exhibited the same change trend as SBH. The evolution of the electronic characteristics can be explained by these parameter changes. The ideal factor n does not change significantly, with or without considering of series resistance in the calculation method. At other temperatures, similar results were obtained. Some of the electronic characteristics of devices irradiated by HIs changed even though the energy of the ions was not very high. These changes might cause devices to function abnormally when applied in aerospace. The explanation of these phenomena will be given in the following chapters.

Table 1
Calculated n, n_r, R_s SBH, and N_D values at 300 K for the 3 fluences.

	1E13 (cm^{-2})	1E14 (cm^{-2})	1E15 (cm^{-2})
n	1.026	1.028	1.021
n_r	1.014	1.010	1.003
R_S [Ohm]	106.51	107.94	108.97
N_D [/cm^3]	3.76E15	3.90E15	5.77E15
$SBH_{C\text{-}V}$ [eV]	2.831	3.329	5.987
$SBH_{I\text{-}V}$ [eV]	1.302	1.325	1.334

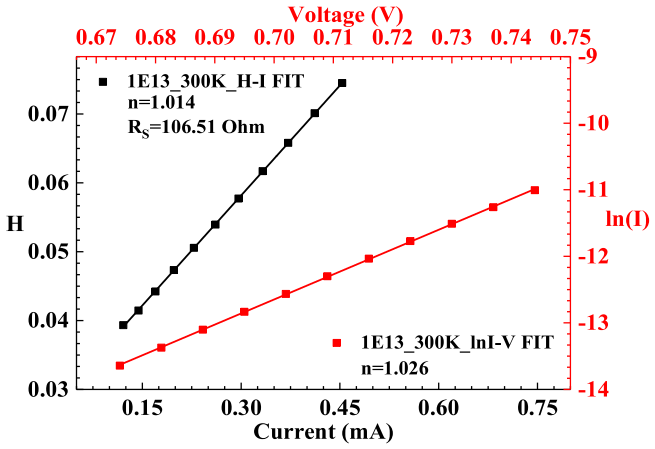

Fig. 3. The fit plot of the forward I-V result at 300 K. ln(I)-V fit drawn in red and H-I fit drawn in black. (For interpretation of the references to colour in this figure legend, the reader is referred to the web version of this article.)

3.3. Results of C-V at different temperature

C-V measurements were determined within the temperature range of 20 K to 500 K. The capacitance at different temperature and irradiation fluences are shown in Fig. 4, and were measured at zero voltage bias and reverse bias at 10 V. Fig. 5. shows the N_D and SBH calculated by Eq. (1) and the fit range was from minus 10 to minus 5. Table 2 shows the fit results at 300 K for each range of 1 V, from minus 1 to minus 10. From the results presented in Table 2, similar effects of radiation were observed for all 10 voltages. Radiation may cause increases of both N_D

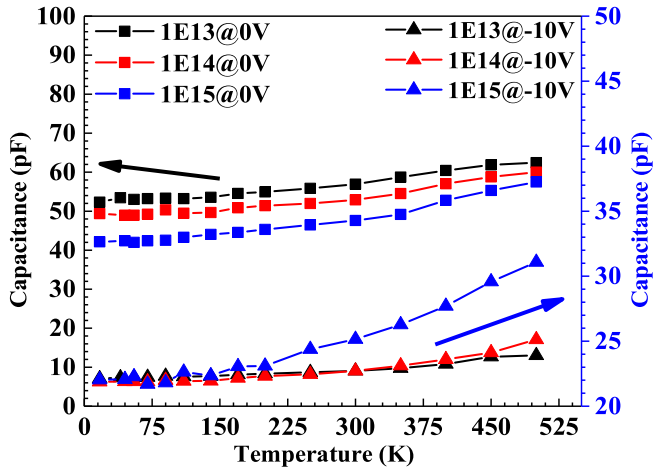

Fig. 4. The capacitance at zero and minus 10 V at different temperatures and fluences.

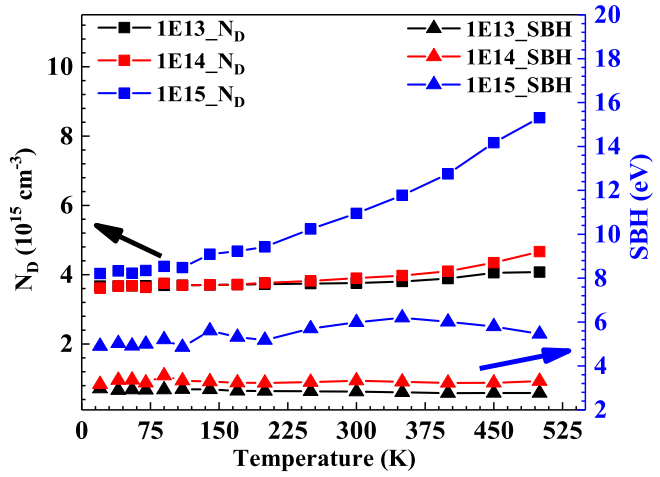

Fig. 5. N_D and SBH extracted from the C-V at different temperatures and fluences.

and $SBH_{c\text{-}v}$ at whatever reverse voltage applied.

At lower temperature, the reverse capacitance properties of all 3 fluences increased slightly with the increased temperature, but at higher temperature, the capacitance increased obviously with temperature, and especially at higher fluences, this increase occurred more rapidly. At reverse bias voltage, the defects in the body substrate have bigger effects on the capacitance. These defects had donor-like properties, causing the increase of the N_D, and as the temperature increased more, more carriers were released from the defects. The extracted values from the linear fit of $1/C^2$-V are shown in Table 2 and verified this point. Radiation always causes an increase in N_D. Additionally, at low temperature, the capacitance was not obviously different for different irradiation fluences when applied as reverse bias, and with increasing temperature, an obvious increase began to occur. At the highest fluence, the capacitance increased rapidly when temperature increased, but at lower fluences of irradiation, this increase with temperature was much slower. At reverse bias and higher temperature (>200 K), the capacitance of the highest fluence was larger than the others, but at zero bias, capacitance was always decreasing as the radiation fluence increasing. The changes of the capacitance with temperature are not as rapid as that at reverse bias, and radiation causes a decrease of the capacitance. At zero or lower reverse bias, it is nearer to the metal/SiC interface, which means greater effects of the defects from the interface. At this condition, the $SBH_{C\text{-}V}$ contributes more to the capacitance. Based on these phenomena, the following conclusions are reached.

1. Defects are induced by HI irradiation, and higher fluences have bigger effects on these defects. This is based on the change of electronic characteristics and the extracted parameters due to the radiation.
2. There are defects both in the body substrate of the SiC material and at the metal/SiC contact interface. In Fig. 3, we can see that the capacitance of zero bias and reverse bias voltage show different change tendencies. Obviously, with the bias voltage in the reverse direction, the depletion region extends more to the body substrate, which means the effects from the interface would become weaker. The N_D and $SBH_{C\text{-}V}$ increase synchronously with the fluence of the radiation for each region of reverse range of voltage, as shown in Table 2. However, according to Eq. (1), these two parameters have opposite effects on the capacitance. Capacitance increases with the N_D and decreases with $SBH_{C\text{-}V}$, so, the capacitance might be affected by both body defects and interface defects. Body defects work like donor centers, causing an increase of N_D, which could enhance the increase of the capacitance and have a bigger effect when reverse voltage is applied. Similarly, defects at the interface might have a positive effect on the $SBH_{C\text{-}V}$, causing a decrease in the capacitance and playing the dominant role at bias voltage close to zero.
3. Defects in the body substrate work like donor centers, and these defects are sensitive to temperature, as shown by negligible effects at lower temperatures but bigger effects at higher temperatures. At low temperature, large parts of the carriers from the body defects are frozen at their energy level, so negligible change occur for different radiation fluences when the temperature is low. In a previous study of HIs at high energy (200 MeV Ag) [16], the defects always exhibit acceptor-like activity, and cause a decrease of N_D. However, in this experiment using HIs at much lower energy, increases of N_D and donor-like defects were observed. It is difficult for Au ions at 6 MeV to penetrate into the SiC layer, which might explain the difference in effect. Simulation by Geant4 revealed that the incidence range of Au ions at 6 MeV is about 2074 nm, and 4 μm of Al layer stopped nearly all the ions.

Table 2
The calculated N_D and $SBH_{c\text{-}v}$ at voltage ranging from −10 to −1V, steps of 1V.

	1E13_N_D (cm^{-3})	1E14_N_D (cm^{-3})	1E15_N_D (cm^{-3})	1E13_SBH (eV)	1E14_SBH (eV)	1E15_SBH (eV)
[−1V,0V]	3.095E+15	3.15E+15	3.84E+15	1.92338	2.219831	3.206438
[−2V, −1V]	3.296E+15	3.4E+15	4.37E+15	2.08826	2.441592	3.739596
[−3V, −2V]	3.435E+15	3.51E+15	4.77E+15	2.251796	2.579871	4.247802
[−4V, −3V]	3.515E+15	3.64E+15	4.99E+15	2.366303	2.778218	4.553115
[−5V, −4V]	3.643E+15	3.74E+15	5.3E+15	2.588985	2.956818	5.084254
[−6V, −5V]	3.654E+15	3.77E+15	5.37E+15	2.609741	3.040953	5.209963
[−7V, −6V]	3.718E+15	3.83E+15	5.66E+15	2.757922	3.171545	5.786482
[−8V, −7V]	3.781E+15	3.84E+15	5.9E+15	2.915819	3.201609	6.322635
[−9V, −8V]	3.763E+15	3.96E+15	5.67E+15	2.859954	3.515604	5.765799
[−10V, −9V]	3.797E+15	3.97E+15	5.92E+15	2.956245	3.547238	6.386055

4. Defects at *the interface could have positive effects on SBH, and these defects seem insensitive to temperature, based on the SBH results from the lower two fluences. Though there are changes in the SBH results at the highest fluence, the change is not very drastic and could be attributed to the rapidly change of N_D. The rapid change of N_D would affect the E_C-E_F in Eq. (1), causing the change of the SBH_{C-V}.

3.4. Results of I-V at different temperature

I-V-T measurements were performed in the temperature range from 20 K to 500 K, and the results are plotted in Fig. 6. By using Eq. (3), the SBH_{I-V}, n factor, and series resistance (R_S) were obtained with assuming Richardson constant of 146 $Acm^{-2}K^{-2}$, and the results are plotted in the Figs. 7–9 below, respectively. V_T is the voltage drop when the current reached 1 mA. For forward or reverse I-V, the current appears to increase as temperature increasing, which is in accordance with the theory of thermionic emission–diffusion (TED). First, in Fig. 8, the change of SBH_{I-V} versus temperature could be due to the barrier inhomogeneity at the Schottky metal/semiconductor interface [19–22]. The SBH_{I-V} and the SBH_{C-V} were not always the same, and the SBH_{C-V} was much higher than that calculated from I to V. This phenomenon may be explained by surface inhomogeneity, quantum mechanical tunneling, interfacial layer and states, mirror force, and edge leakage currents [23]. The presence of a thin layer between the metal/SiC interfaces might also cause differences between SBH_{I-V} and SBH_{C-V}. Also, the SBD might correspond to several SBH, explaining why different SBH values can be extracted when applying different voltages [24]. Both SBH_{I-V} and R_S increase with increasing temperature and irradiation fluence, but V_T shows the opposite tendency. The n factor values extracted with or without considering resistance decreased rapidly at lower temperatures (<150 K) and then changed weakly as the temperature increased, suggesting that the Thermal Emission (TE) model was not appropriate for low temperature and that generation-recombination was dominant [10]. The increase of R_S might be due to the decrease of the mobility of the carriers due to impurity scattering. Finally, with increasing temperature, phonon scattering would cause further increase in R_S.

Fig. 10 shows the current at bias voltages of 0.4 V and minus 50 V. As shown, the current versus temperature and irradiation fluence exhibits a different tendency between forward and reverse bias. At reverse bias voltage, there was a negligible difference at low temperature and low radiation fluence is low (<200 K), but the reverse current increased more at higher temperature. Especially, for the device under higher fluence of radiation, the reverse current always increased significantly at all temperatures. Similar results were observed for the forward current. As discussed above for the C-V, the rapid increase of N_D can explain the change for the reverse current. The higher N_D value causes a greater

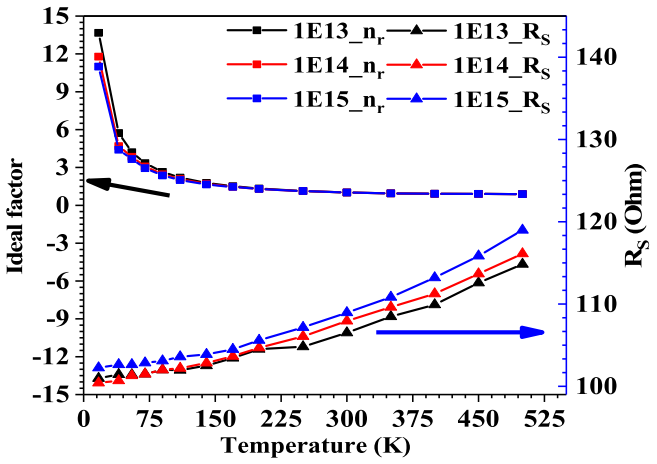

Fig. 7. Ideal factor calculated using series resistance; R_S versus temperature.

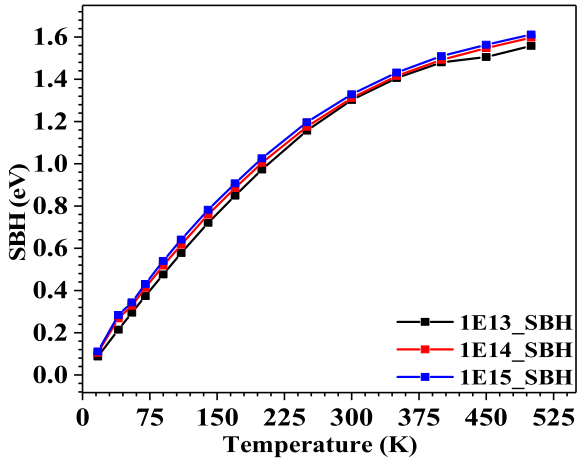

Fig. 8. SBH_{I-V} versus Temperature.

decrease in SBH due to the image force and tunneling effect, which agrees excellently with the results of current under reverse bias. Fig. 11 shows the evolution of the current with increasing voltage. Compared with the results at bias voltage of 0.2 V, the current under lower fluence radiation is larger, and this effect is more obvious at higher bias voltage and higher temperature. The current should increase with temperature, so the following effects would be induced by radiation. For the forward current, two mechanisms can together affect the I-V characteristics:

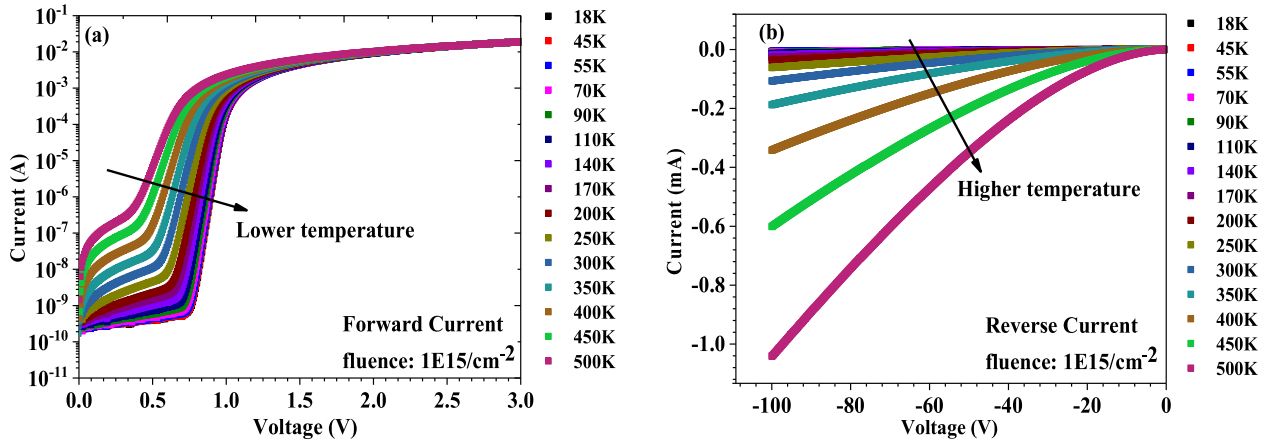

Fig. 6. (a) Semi ln(I)-V-T and (b) reverse I-V-T.

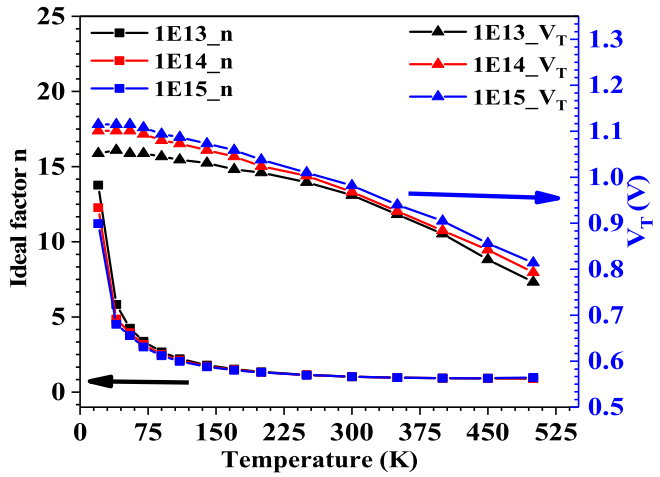

Fig. 9. Ideal factor n and V_T versus temperature.

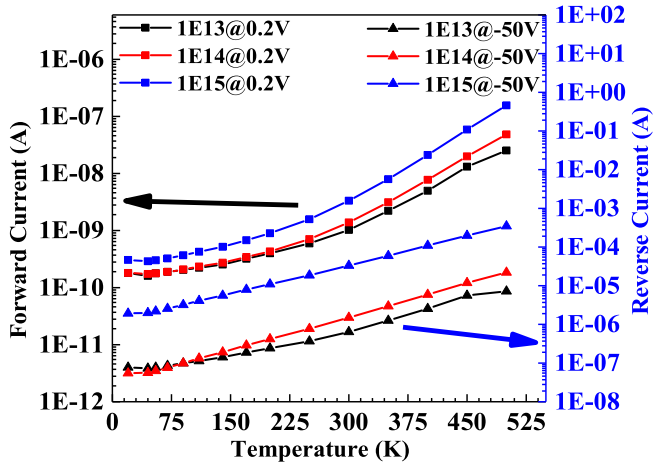

Fig. 10. The semi-log current at bias voltage at 0.2 V and minus 50 V.

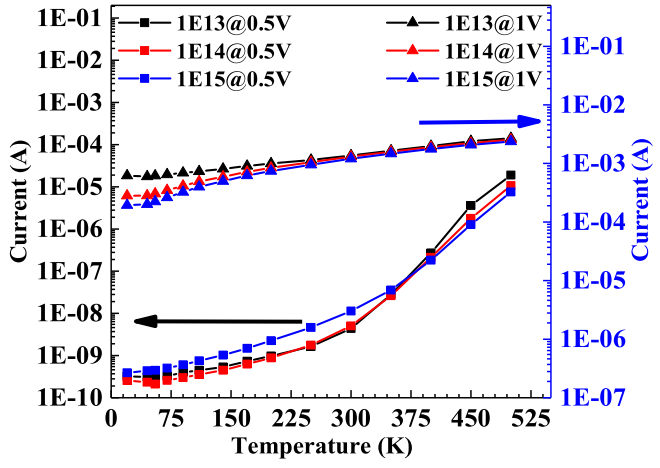

Fig. 11. The semi-log current at bias voltage at 0.5 V and 1 V.

thermal emission diffusion (TED) and generation-recombination (GR). According to the results in Figs. 10 and 11, at lower voltage, N_D may be more important in carrier transport, which promoting the diffusion current to explain why higher N_D could cause the current increasing. Based on the change tendency of N_D shown in Fig. 5, the current shows a similar trend. Additionally, the recombination center induced by radiation could lead to the increase of the GR current created by de-trapping when the current is low [25]. We calculated the ideal factor at low forward bias voltage (~0.2 V) to test this explanation, with 8.46, 9.16, and 8.06 for the 3 fluences at 300 K and 6.14, 6.10, and 5.57 at 400 K, respectively. The n factors deviate to 1 much, which means the GR current makes a bigger contribution and the TED model is not appropriate for this low voltage condition. However, with increasing bias voltage, the TED model becomes dominant, as the higher $SBH_{I\text{-}V}$ causes the current to decrease a little. Also, when the current increases, the effects of series resistance cannot be ignored. The evolution of the R_S and SBH are shown in Figs. 7 and 8 is consistent with the slight current decrease.

4. Conclusion

Based on the results and discussion, the following conclusions can be reached. Now some points would be summarized below:

Irradiation might induce both body and interface defects, affecting N_D and $SBH_{C\text{-}V}$, respectively. Body defects can act as donor centers and are sensitive to temperature. The interface defects are less sensitive to temperature, and might be slightly affected by high dosage concentration. High doping concentration plays important roles in the reverse I-V characteristics, causing the current to increase by image force and tunneling effect, which decrease the SBH. Also, with GR effects, defects cause an increase in forward current at lower voltage. Irradiation causes a decrease in the n factor at low temperature, but there is little effect at little higher temperature. At the same time, the series resistance and $SBH_{I\text{-}V}$ increased with irradiation, causing effects at higher voltage and leading to current decrease and V_T increase. The increase of R_S might be due to the decrease of carrier mobility due to impurity scattering.

Temperature also can affect the electronic parameters of the Schottky SBD. Body defects induced by radiation function as donor centers and these effects strengthen with increasing temperature. The $SBH_{C\text{-}V}$ does not change a lot with temperature, but $SBH_{I\text{-}V}$ increases with temperature due to the inhomogeneous barrier. The n factor decreases rapidly at low temperature and then stabilizes, suggesting the TED model is not appropriate to explain behavior at low temperature. Instead, generation-recombination is the dominant effect.

HIs irradiation causes little change in $SBH_{I\text{-}V}$ or n factor, but obvious changes in R_S, V_T, and N_D. These changes severely influence the electronic properties of devices when exposed to HIs radiation, especially high fluence radiation. Temperature can significantly affect the electronic properties of Schottky SBD, and by inducing interface and body defects, changes can be intensified and finally affect the overall reliability of these devices when functioning in an aerospace environment that is with rich of radiation and experiences a large range of temperature change.

CRediT authorship contribution statement

Duowei Wang: Conceptualization, Methodology, Formal analysis, Investigation, Visualization, Writing - original draft. **Rongbin Hu:** Investigation, Formal analysis. **Gang Chen:** Investigation, Formal analysis. **Changqin Tang:** Conceptualization, Methodology. **Yao Ma:** Conceptualization, Resources, Writing - review & editing. **Min Gong:** Writing - review & editing, Supervision. **Qingkui Yu:** Methodology, Investigation. **Shuang Cao:** Methodology, Investigation. **Yun Li:** Methodology, Investigation, Data curation, Project administration. **Mingmin Huang:** Software, Writing - review & editing. **Zhimei Yang:** Conceptualization, Writing - review & editing, Supervision, Funding acquisition.

Declaration of Competing Interest

The authors declare that they have no known competing financial interests or personal relationships that could have appeared to influence

the work reported in this paper.

Acknowledgements

This project is supported by the National Key R&D Plan through Grant No. 2017YFB0405702, the National Natural Science Foundation of China under Grant No. 61704116 and 11875068, the fund of Innovation Center of Radiation Application under Grant No. KFZC2020021001 and Science and Technology on Analog Integrated Circuit Laboratory under Grant No. 6142802190505.

References

[1] J.L. Hudgins, Wide and narrow bandgap semiconductors for power electronics: a new valuation, J. Electron. Mater. 32 (6) (2003) 471–477.
[2] R. Singh, Reliability and performance limitations in SiC power devices, Microelectron. Reliab. 46 (5-6) (2006) 713–730.
[3] E. Omotoso, W.E. Meyer, S.M.M. Coelho, et al., Electrical characterization of defects introduced during electron beam deposition of W Schottky contacts on n-type 4H-SiC, Mater. Sci. Semicond. Process. 51 (2016) 20–24.
[4] F. Moscatelli, A. Scorzoni, A. Poggi, et al., Measurements and simulations of charge collection efficiency of p+/n junction SiC detectors, Nucl. Instrum. Methods Phys. Res. A 483–485 (2005) 1021–1024.
[5] L. JeanMarie, C. Megan, T. Alyson, et.al., Silicon Carbide Power Device Performance Under Heavy-Ion Irradiation, NASA/Langley Research Center, Jul 16, (2015).
[6] M. Gong, S. Fung, C.D. Beling, et al., A deep level transient spectroscopy study of electron irradiation induced deep levels in p-type 6H–SiC, J. Appl. Phys. 85 (1999) 7120–7122.
[7] K. Çınar, C. Coşkun, Ş. Aydoğan, H. Asıl, E. Gür, The effect of the electron irradiation on the series resistance of Au/Ni/6H-SiC and Au/Ni/4H-SiC Schottky contacts, Nucl. Instrum. Methods Phys. Res. B 268 (6) (2010) 616–621.
[8] J. Garcia Lopez, M.C. Jimenez-Ramos, M. Rodriguez-Ramos, J. Ceballos, F. Linez, J. Raisanen, Comparative study by IBIC of Si and SiC diodes irradiated with high energy protons, Nucl. Instrum. Methods Phys. Res. B 372 (2016) 143–150.
[9] B. Tsuchiya, T. Shikama, S. Nagata, K. Saito, T. Nozawa, Dynamic measurements of radiation-induced electrical-property modifications in CVD-SiC under fast neutron irradiation, J. Nucl. Mater. 455 (1-3) (2014) 645–648.
[10] E. Omotoso, W.E. Meyer, F.D. Auret, et al., Effects of 5.4 MeV alpha-particle irradiation on the electrical properties of nickel Schottky diodes on 4H-SiC, Nucl. Instrum. Methods Phys. Res. B 365 (2015) 264–268.
[11] E. Omotoso, W.E. Meyer, F.D. Auret, et al., Electrical characterization of deep levels created by bombarding nitrogen-doped 4H-SiC with alpha-particle irradiation, Nucl. Instrum. Methods Phys. Res. B 371 (2016) 312–316.
[12] A.T. Paradzah, F.D. Auret, M.J. Legodi, et al., Electrical characterization of 5.4 MeV alpha-particle irradiated 4H-SiC with low doping density, Nucl. Instrum. Methods Phys. Res. B 358 (2015) 112–116.
[13] T. Makino, M. Deki, N. Iwamoto, S. Onoda, N. Hoshino, H. Tsuchida, T. Hirao, T. Ohshima, Heavy-ion induced anomalous charge collection from 4H-SiC schottky barrier diodes, IEEE Trans. Nucl. Sci. 60 (4) (2013) 2647–2650.
[14] C. Abbate, G. Busatto, P. Cova, N. Delmonte, F. Giuliani, F. Iannuzzo, A. Sanseverino, F. Velardi, Thermal damage in SiC Schottky diodes induced by SE heavy ions, Microelectron. Reliab. 54 (9-10) (2014) 2200–2206.
[15] C. Kamezawa, H. Sindou, T. Hirao, H. Ohyama, S. Kuboyama, Heavy ion-induced damage in SiC Schottky barrier diode, Phys. B Condensed Matter 376-377 (2006) 362–366.
[16] V. Kumar, A.S. Maan, J. Akhtar, Tailoring surface and electrical properties of Ni/4H-nSiC Schottky barrier diodes via selective swift heavy ion irradiation, Phys. Status Solidi 215 (5) (2018) 1700555, https://doi.org/10.1002/pssa:v215.510.1002/pssa:201700555.
[17] Z.M. Yang, Y. Li, Y. Ma, et al., XTEM investigation of recovery on electrical degradation of 4H-SiC Schottky barrier diode by swift heavy ^{209}Bi ions irradiation, Nucl. Instrum. Methods Phys. Res. B 407 (2017) 304–309.
[18] J.F. Han, Z. An, G. Zheng, et al., An ion beam facility based on a 3 MV tandetron accelerator in Sichuan University, China, Nucl. Instrum. Methods Phys. Res. B Beam Interact. Mater. Atoms 418 (2018) 68–73.
[19] A. Jayawardena, A.C. Ahyi, S. Dhar, Analysis of temperature dependent forward characteristics of Ni/-201Ga_2O_3 Schottky diodes, Semicond. Sci. Technol. 31 (2016), 115002.
[20] S.K. Cheung, N.W. Cheung, Extraction of Schottky diode parameters from forward current-voltage characteristics, Appl. Phys. Lett. 49 (2) (1986) 85–87.
[21] M. Cakar, N. Yildirim, S. Karatas, et al., Current-voltage and capacitance-voltage characteristics of Sn/rhodamine-and Sn/rhodamine- Schottky barrier diodes, J. Appl. Phys. 100 (2006), 074505.
[22] Q. Feng, Z. Feng, Z. Hu, X. Xing, G. Yan, J. Zhang, Y. Xu, X. Lian, Y. Hao, Temperature dependent electrical properties of pulse laser deposited Au/Ni/β-(AlGa)2O3 Schottky diode, Appl. Phys. Lett. 112 (7) (2018) 072103, https://doi.org/10.1063/1.5019310.
[23] C. Raynaud, K. Isoird, M. Lazar, et al., Barrier height determination of SiC Schottky diodes by capacitance and current–voltage measurements, J. Appl. Phys. 91 (2002) 9841–9847.
[24] E. Omotoso, W.E. Meyer, F.D. Auret, et al., The influence of high energy electron irradiation on the Schottky barrier height and the richardson constant of Ni/4H-SiC schottky diodes, Mater. Sci. Semicond. Process. 39 (2015) 112–118.
[25] S. Kumar, Y.S. Katharria, V. Baranwal, et al., Inhomogeneities in 130MeV Au^{12+} ion irradiated Au/n-Si (100) Schottky structure, Appl. Surf. Sci. 254 (2008) 3277–3281.